ChemPubSoc Europe

DOI: 10.1002/chem.201501717

CHEMISTRY
A European Journal
Full Paper

Cavitands |*Hot Paper*|

# Self-Assembled Boronic Ester Cavitand Capsules with Various Bis(catechol) Linkers: Cavity-Expanded and Chiral Capsules

Kento Tamaki,[a] Asumi Ishigami,[a] Yasutaka Tanaka,[b] Masamichi Yamanaka,[a] and Kenji Kobayashi*[a]

**Abstract:** Two molecules of cavitand tetraboronic acid and four molecules of various bis(catechol) linkers self-assemble into capsules through the formation of eight dynamic boronic ester bonds. Each capsule has a different cavity size depending on the linker used, and shows particular guest encapsulation selectivity. A chiral capsule made up of the cavitand and a chiral bis(catechol) linker was also constructed. This capsule induces supramolecular chirality with respect to a prochiral biphenyl guest by diastereomeric encapsulation through the asymmetric suppression of rotation around the axis of the prochiral biphenyl moiety.

## Introduction

Supramolecular capsules, constructed by self-assembly of preorganized subunits, provide an isolated nanospace. Guest molecules confined in the nanospace often show unique properties that are not observed in their free forms. Calix[4]resorcinarene cavitands are valuable subunits for covalent-bonded capsules,[1] as well as self-assembled capsules under thermodynamic control using noncovalent interactions, such as hydrogen bonds,[2] metal-coordination bonds,[3] ionic interactions,[4] and solvophobic interactions.[5] As an alternative strategy, dynamic covalent chemistry offers great advantages in supramolecular syntheses because dynamic covalent bonds undergo reversible covalent bond-forming and bond-breaking processes that are under thermodynamic control; namely, such connections combine both the strength of covalent bonds and the reversibility of noncovalent interactions.[6,7] The reversibility of the imine bond-forming reaction in the presence of a catalytic amount of $CF_3CO_2H$[7b,8] or the disulfide bond-forming reaction under redox buffer conditions[9] has been applied to cavitand-based capsule synthesis. Boronic ester formation is another reliable synthon for dynamic covalent chemistry.[10] The merit of boronic ester formation is that there is no requirement for the addition of external chemicals to the system. Capsule syntheses using various types of subunits based on the reversible formation of boronic or boronate esters have been reported recently.[11]

Chiral capsules are another interesting topic in supramolecular nanospace chemistry. Chiral molecular recognition of a racemic guest upon encapsulation in chiral capsules has been studied extensively.[12–14] In a type of twisted capsule composed of north and south hemispheres,[15] it is known that the equilibrium between (*P*)- and (*M*)-twistomers can be controlled either by the introduction of a chiral group onto a racemic self-assembled capsule[14b] or by the encapsulation of a chiral guest into a racemic self-assembled capsule.[16] Chiral induction of a prochiral guest upon encapsulation in a chiral capsule would also be important for supramolecular nanospace chemistry because such an encapsulation design is related to asymmetric capsular catalysts[17] and to the emergence of novel stereoisomerisms.[18] Dynamic covalent-bonded chiral capsules have been reported;[19] however, chiral encapsulation in such capsules has not been studied so far, probably due to the formidable challenges of molecular design.

Previously, we reported that two molecules of cavitand tetraboronic acid **1**, as a polar aromatic cavity end, and four molecules of 1,2-bis(3,4-dihydroxyphenyl)ethane **E**, as an equatorial bis(catechol)-linker, self-assemble into capsule $\mathbf{1}_2\mathbf{E}_4$ through the formation of eight dynamic boronic ester bonds (Figure 1 a).[20] Capsule $\mathbf{1}_2\mathbf{E}_4$ encapsulates a guest molecule, such as 4,4′-disubstituted-biphenyl derivatives, to form guest@$\mathbf{1}_2\mathbf{E}_4$ in a selective recognition event, wherein the guest substituents are oriented to both aromatic cavity ends of $\mathbf{1}_2\mathbf{E}_4$ so as to maximize capsule–guest interactions. If various bis(catechol) linkers are available for capsular assembly with **1** in place of **E**, this strategy would endow the self-assembled boronic ester cavitand capsule with an increased range of applications, such as a cavity-expanded capsule[8b,11c,21,22] for larger guest encapsulation, or a chiral capsule[19] for chiral sensing technology. Herein, we report on cavity-expanded boronic ester cavitand capsules self-assembled by **1** and various bis(catechol) linkers, which

[a] *K. Tamaki, A. Ishigami, Prof. M. Yamanaka, Prof. K. Kobayashi*
*Department of Chemistry, Faculty of Science*
*Shizuoka University, 836 Ohya, Suruga-ku*
*Shizuoka 422-8529 (Japan)*
*E-mail: kobayashi.kenji.a@shizuoka.ac.jp*

[b] *Prof. Y. Tanaka*
*Department of Electronics and Materials Science*
*Faculty of Engineering, Shizuoka University*
*3-5-1 Johoku, Naka-ku, Hamamatsu 432-8561 (Japan)*

*Supporting information for this article is available on the WWW under http://dx.doi.org/10.1002/chem.201501717.*

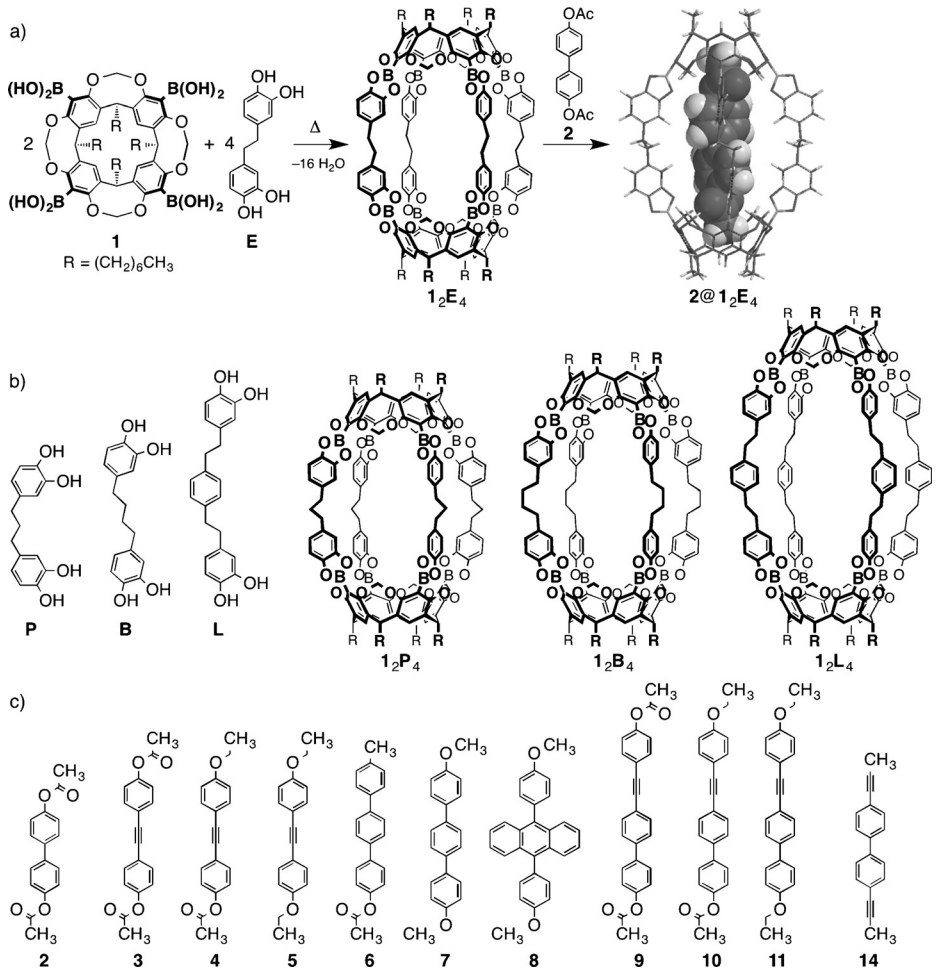


**Figure 1.** a) Self-assembly of cavitand tetraboronic acid **1** and bis(catechol) linker **E** into capsule $\mathbf{1}_2\mathbf{E}_4$ and the molecular model of guest-encapsulating capsule $\mathbf{2}@\mathbf{1}_2\mathbf{E}_4$.[20b] b) Bis(catechol) linkers **P**, **B**, and **L**, and their capsules $\mathbf{1}_2\mathbf{P}_4$, $\mathbf{1}_2\mathbf{B}_4$, and $\mathbf{1}_2\mathbf{L}_4$. c) Guest molecules **2**–**11** and **14** investigated in this study.

show particular guest encapsulation selectivity depending on the capsule size. We also describe a chiral capsule, composed of **1** and a chiral bis(catechol) linker, which expresses diastereomeric encapsulation selectivity with respect to a prochiral biphenyl guest by asymmetric suppression of axial rotation of the biphenyl moiety upon encapsulation.

## Results and Discussion

### Capsule formation from cavitand tetraboronic acid and bis(catechol) linkers

We selected 1,3-bis(3,4-dihydroxyphenyl)propane (**P**),[23] 1,4-bis(3,4-dihydroxyphenyl)butane (**B**),[23] and 1,4-bis[2-(3,4-dihydroxyphenyl)ethyl]benzene (**L**) (see the Supporting Information), as flexible bis(catechol) linkers. The reaction for a 2:4 mixture of cavitand tetraboronic acid **1** with bis(catechol) linker **P**, **B**, or **L** in $CDCl_3$ at 50 °C produced the self-assembled capsules $\mathbf{1}_2\mathbf{P}_4$, $\mathbf{1}_2\mathbf{B}_4$, and $\mathbf{1}_2\mathbf{L}_4$, respectively, quantitatively as single species (Figure 1b).[24] The $^1$H NMR spectra of capsules $\mathbf{1}_2\mathbf{P}_4$, $\mathbf{1}_2\mathbf{B}_4$, and $\mathbf{1}_2\mathbf{L}_4$ in $C_6D_6$ are shown in Figure 2 (for $^1$H NMR spectra of the compounds in $CDCl_3$, see Figure S9 in the Supporting Information). In a manner similar to the formation of capsule $\mathbf{1}_2\mathbf{E}_4$,[20] each $^1$H NMR spectrum showed a highly symmetrical single species and confirmed the disappearance of the OH groups of the units **1**, **P**, **B**, and **L**, indicating quantitative formation of capsules $\mathbf{1}_2\mathbf{P}_4$, $\mathbf{1}_2\mathbf{B}_4$, and $\mathbf{1}_2\mathbf{L}_4$, respectively. Each capsule could be isolated by reprecipitation from benzene–hexane.

### Guest encapsulation

Each capsule has a different cavity size that depends on the linker used, and each encapsulates one guest molecule in $C_6D_6$, with particular guest encapsulation selectivity. The guest encapsulation was slow and required approximately 0.5–1 day to reach thermodynamic equilibration at room temperature. The catalytic amount of water that is inevitably present in $C_6D_6$ led to reversibility of the boronic ester bond, partial capsule opening, and guest encapsulation within the capsules.[20b] Guest molecules **2**–**11**, which were investigated here, are shown in Figure 1c. Representative $^1$H NMR spectra of guests@capsules are shown in Figure 3 (for other guests@capsules, see Figure S10–S21 in the Supporting Information). The $^1$H NMR signals of encapsulated and free guests were independently observed, and the signals of the terminal methyl protons of functional groups of the encapsulated guests were shifted upfield by 2.28–3.01 ppm relative to those of free guests in $C_6D_6$, because of the ring-current effect of the aromatic cavities of capsules. These results indicate that the functional groups of all guests encapsulated within the capsules are oriented toward the aromatic cavity ends of the capsules, in a manner similar to guest@$\mathbf{1}_2\mathbf{E}_4$.[20] The apparent association constants ($K_{app}$) of capsules $\mathbf{1}_2\mathbf{P}_4$, $\mathbf{1}_2\mathbf{B}_4$, and $\mathbf{1}_2\mathbf{L}_4$ with various guests in $C_6D_6$ at 25 °C,[25] and the changes in $^1$H NMR chemical shifts of the terminal methyl protons of the functional groups in the guests@capsules relative to those of the free guests ($\Delta\delta_G = \delta_{encapsulated\text{-}guest} - \delta_{free\text{-}guest}$) are summarized in Table 1.

The encapsulation of 4,4′-diacetoxybiphenyl **2** in $\mathbf{1}_2\mathbf{P}_4$ showed $K_{app} = 4.98 \times 10^3\ M^{-1}$ and $\Delta\delta_G = -3.00$ ppm, whereas $\mathbf{2}@\mathbf{1}_2\mathbf{E}_4$ exhibited $K_{app} = 1.26 \times 10^6\ M^{-1}$ and $\Delta\delta_G = -2.85$ ppm[20b] (Table 1, entries 3 vs. 1, and Figure 3b vs. 3a). The smaller $K_{app}$ and larger upfield shift of $\Delta\delta_G$ of $\mathbf{2}@\mathbf{1}_2\mathbf{P}_4$ compared with the

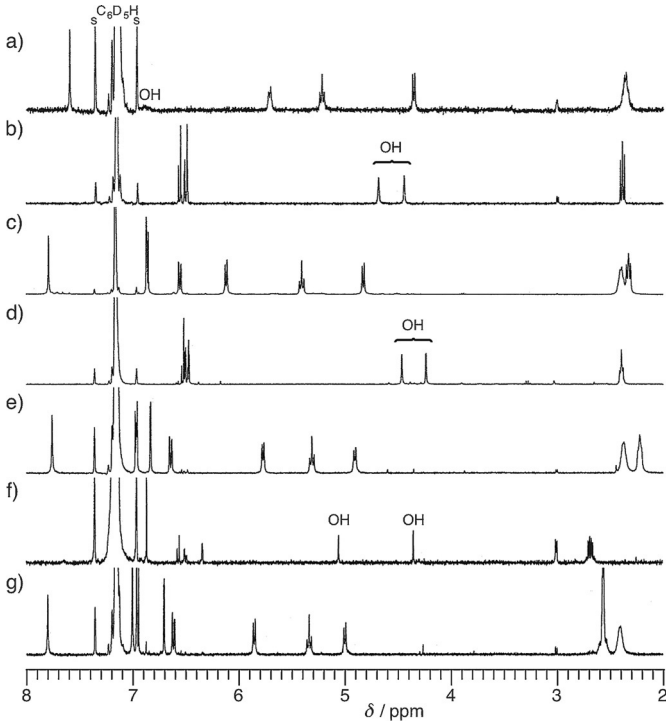


**Figure 2.** $^1$H NMR spectra (400 MHz, $C_6D_6$, 298 K) of a) **1** (heterogeneous); b) **P** (heterogeneous); c) $\mathbf{1}_2\mathbf{P}_4$; d) **B** (heterogeneous); e) $\mathbf{1}_2\mathbf{B}_4$; f) **L** (heterogeneous); and g) $\mathbf{1}_2\mathbf{L}_4$. The signals marked 's' are the satellite signals ($^{13}$C-$^1$H coupling) of the residual solvent.

**Table 1.** Apparent association constants ($K_{app}$) of capsules $\mathbf{1}_2\mathbf{P}_4$, $\mathbf{1}_2\mathbf{B}_4$, and $\mathbf{1}_2\mathbf{L}_4$ with guests, and the $^1$H NMR chemical shift changes ($\Delta\delta_G$) of guest@capsule relative to free guests at the terminal methyl protons in $C_6D_6$ at 298 K.

| Entry | Capsule | Guest | $K_{app}$ [M$^{-1}$][a] | $\Delta\delta_G$ [ppm][b] |
|---|---|---|---|---|
| 1[c] | $\mathbf{1}_2\mathbf{E}_4$ | **2** | $1.26\times10^6$ | −2.85 |
| 2 | $\mathbf{1}_2\mathbf{E}_4$ | **3** | ≈0 | |
| 3 | $\mathbf{1}_2\mathbf{P}_4$ | **2** | $4.98\times10^3$ | −3.00 |
| 4 | $\mathbf{1}_2\mathbf{P}_4$ | **3** | ≈0 | |
| 5 | $\mathbf{1}_2\mathbf{B}_4$ | **2** | ≈0 | |
| 6 | $\mathbf{1}_2\mathbf{B}_4$ | **3** | $2.45\times10^5$ | −2.88 |
| 7 | $\mathbf{1}_2\mathbf{B}_4$ | **4** | $1.38\times10^4$ | −2.89,[d] −2.89[e] |
| 8 | $\mathbf{1}_2\mathbf{B}_4$ | **5** | $1.53\times10^3$ | −2.89 |
| 9 | $\mathbf{1}_2\mathbf{B}_4$ | **6** | $4.31\times10^3$ | −2.96,[d] −2.96[f] |
| 10 | $\mathbf{1}_2\mathbf{B}_4$ | **7** | $4.20\times10^2$ | −2.34 |
| 11 | $\mathbf{1}_2\mathbf{B}_4$ | **8** | $4.48\times10^3$ | −2.28 |
| 12 | $\mathbf{1}_2\mathbf{L}_4$ | **9** | $4.18\times10^6$ | −2.89, −2.83 |
| 13 | $\mathbf{1}_2\mathbf{L}_4$ | **10** | $2.05\times10^5$ | −2.93,[d] −2.85[e] |
| 14 | $\mathbf{1}_2\mathbf{L}_4$ | **11** | $8.59\times10^3$ | −3.01, −2.92 |

[a] $K_{app}=[G@Capsule]/\{[Capsule]_f[G]_f\}$ or $K_{app}/K_{app\text{-}Standard}=\{[G@Capsule][G_{Standard}]_f\}/\{[G_{Standard}@Capsule][G]_f\}$. Errors are within 10%. [b] $\Delta\delta_G=\delta_{encapsulation\text{-}guest}-\delta_{free\text{-}guest}$. [c] See ref. [20b]. The $K_{app}$ value was measured at 313 K. [d] Acetoxy group. [e] Ethoxy group. [f] Methyl group.

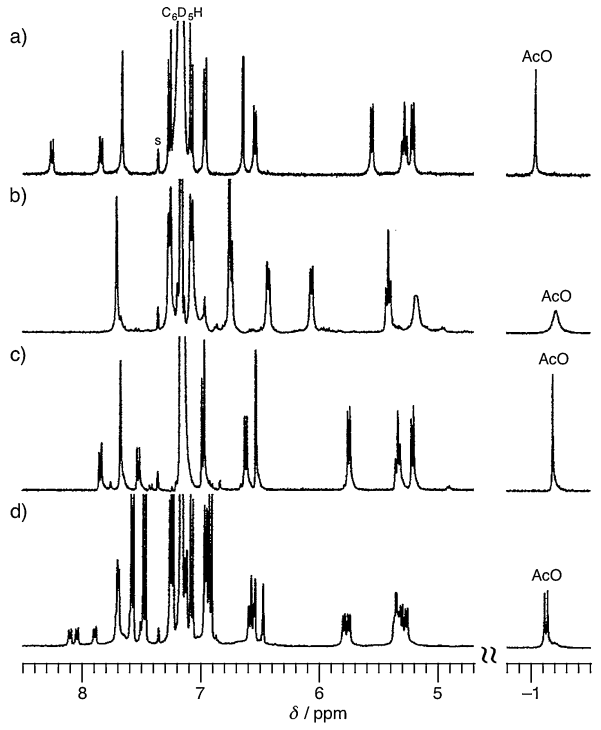


**Figure 3.** $^1$H NMR spectra (400 MHz, $C_6D_6$, 298 K) of representative guest@capsule: a) $\mathbf{2}@\mathbf{1}_2\mathbf{E}_4$ ([$\mathbf{1}_2\mathbf{E}_4$] = 1 mM and [**2**] = 2 mM); b) $\mathbf{2}@\mathbf{1}_2\mathbf{P}_4$ ([$\mathbf{1}_2\mathbf{P}_4$] = 2.5 mM and [**2**] = 7.5 mM); c) $\mathbf{3}@\mathbf{1}_2\mathbf{B}_4$ ([$\mathbf{1}_2\mathbf{B}_4$] = 1 mM and [**3**] = 1 mM); and d) $\mathbf{9}@\mathbf{1}_2\mathbf{L}_4$ ([$\mathbf{1}_2\mathbf{L}_4$] = 1 mM and [**9**] = 5 mM). AcO = Acetoxy signals of the encapsulated guest.

$K_{app}$ and $\Delta\delta_G$ of $\mathbf{2}@\mathbf{1}_2\mathbf{E}_4$ clearly indicate that the cavity size (length) of $\mathbf{1}_2\mathbf{P}_4$ is slightly smaller than that of $\mathbf{1}_2\mathbf{E}_4$.[26,27] Linker **P** is longer than **E**; however, this is not the case for the capsules. In contrast to the *anti*-conformation of linker **E** in $\mathbf{1}_2\mathbf{E}_4$,[20b] linker **P** would adopt a *skew*-conformation to form $\mathbf{1}_2\mathbf{P}_4$. Therefore, the cavity size (length) of $\mathbf{1}_2\mathbf{P}_4$ is slightly smaller than that of $\mathbf{1}_2\mathbf{E}_4$.

Capsules $\mathbf{1}_2\mathbf{B}_4$ and $\mathbf{1}_2\mathbf{L}_4$ possess more expanded cavities than $\mathbf{1}_2\mathbf{E}_4$ and can encapsulate larger guests that are inaccessible for $\mathbf{1}_2\mathbf{E}_4$ (Figure 1b and 1c). Capsule $\mathbf{1}_2\mathbf{B}_4$ encapsulates 4,4′-bis(*p*-substituted-phenyl)acetylenes **3**–**5** (Table 1, entries 6–8, and Figure 3c) and 4,4″-disubstituted-*p*-terphenyls **6**–**8** (Table 1, entries 9–11). Capsule $\mathbf{1}_2\mathbf{L}_4$ encapsulates 4-substituted-4′-(*p*-substituted-phenylethynyl)biphenyls **9**–**11** (Table 1, entries 12–14, and Figure 3d), which are significantly larger in size than **3**–**8**. Thus, the cavity size (length) of capsules increases in the order $\mathbf{1}_2\mathbf{P}_4 \le \mathbf{1}_2\mathbf{E}_4 < \mathbf{1}_2\mathbf{B}_4 < \mathbf{1}_2\mathbf{L}_4$. In a manner similar to $\mathbf{1}_2\mathbf{E}_4$,[20b] capsules $\mathbf{1}_2\mathbf{B}_4$ and $\mathbf{1}_2\mathbf{L}_4$ strictly discriminate between functional groups of a guest. In a series of guests with a similar molecular length, the $K_{app}$ values of guest@$\mathbf{1}_2\mathbf{B}_4$ and guest@$\mathbf{1}_2\mathbf{L}_4$ increased in the order **5** (4,4′-$OCH_2CH_3$) < **4** (4-OC(=O)$CH_3$-4′-$OCH_2CH_3$) < **3** (4,4′-OC(=O)$CH_3$), and **11** < **10** < **9**, respectively. This selectivity arises from a combination of CH···π interaction between the terminal $CH_3$ group of the guest and the electron-rich aromatic cavity end of $\mathbf{1}_2\mathbf{B}_4$ and $\mathbf{1}_2\mathbf{L}_4$, and C=O···HC interaction between the carbonyl oxygen atom of the acetoxy group of the guest and the inner protons of the methylene-bridge rims (O-$CH_{in}H_{out}$-O) of $\mathbf{1}_2\mathbf{B}_4$ and $\mathbf{1}_2\mathbf{L}_4$, which are observed in the X-ray crystal structure of $\mathbf{2}@\mathbf{1}_2\mathbf{E}_4$.[20b]

### Chiral capsules and chiral induction of a prochiral biphenyl guest upon encapsulation: a $^1$H NMR study

Chiral induction of a prochiral guest upon encapsulation in a chiral capsule is important for supramolecular nanospace chemistry, particularly with respect to asymmetric capsular catalysts[17] and for the emergence of novel stereoisomerisms,[18] as well as for chiral materials science.[28] 4,4′-Diacetoxy-2,2′-bis-(methoxycarbonyl)biphenyl (**12**) is a prochiral molecule, but it becomes chiral when rotation around the biphenyl axis is asymmetrically suppressed by chiral steric factors that fix the configuration of the biphenyl moiety asymmetrically.

We studied chiral induction of prochiral **12** upon encapsulation within a chiral $\mathbf{1}_2\mathbf{E}_4$ capsule derivative. Thus, we synthesized racemic 2,3-bis(3,4-dihydroxyphenyl)butane, which was separated by HPLC with a chiral column into the corresponding chiral (2*R*,3*R*)-form $\mathbf{E}^R$ and its enantiomeric (2*S*,3*S*)-form $\mathbf{E}^S$ as chiral bis(catechol)ethane linkers (see the Supporting Information). The absolute configurations of $\mathbf{E}^R$ and $\mathbf{E}^S$ were determined by comparing the observed and theoretical circular dichroism spectra (Figure 9a vs. 9b, see below). The reaction of **1** with chiral $\mathbf{E}^R$ in a 2:4 ratio in $CDCl_3$ at 50 °C produced the self-assembled chiral capsule $\mathbf{1}_2\mathbf{E}^R{}_4$ quantitatively (Figure 4a and 5). In a manner similar to the formation of capsule $\mathbf{1}_2\mathbf{E}_4$,[20a,b] the $^1$H NMR spectrum of the reaction mixture (Figure 5c and Figure S22 in the Supporting Information) indicated the presence of a highly symmetrical single species and confirmed the disappearance of the OH groups of the constituent units **1** and $\mathbf{E}^R$, indicating the quantitative formation of $\mathbf{1}_2\mathbf{E}^R{}_4$. Enantiomeric $\mathbf{1}_2\mathbf{E}^S{}_4$ was synthesized similarly. In contrast, the reaction of **1** with racemic $\mathbf{E}^R$ and $\mathbf{E}^S$ in a 2:2:2 ratio gave a complex mixture without self-sorting of chiral linkers (Figure 5d).[29]

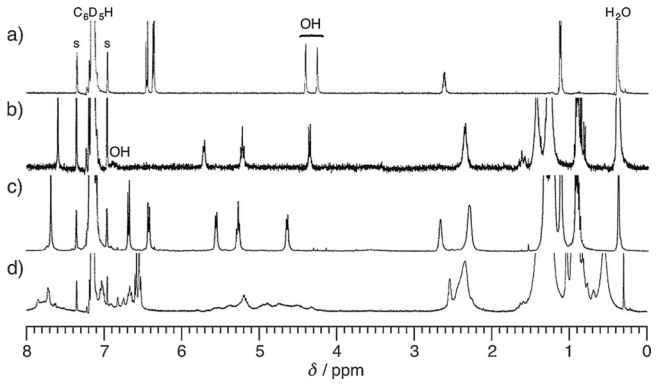


**Figure 5.** $^1$H NMR spectra (400 MHz, $C_6D_6$, 298 K) of a) $\mathbf{E}^R$ (heterogeneous); b) **1** (heterogeneous); c) $\mathbf{1}_2\mathbf{E}^R{}_4$; and d) the reaction mixture of **1** with racemic $\mathbf{E}^R$ and $\mathbf{E}^S$ in a 2:2:2 ratio after heating in $C_6D_6$ at 50 °C for 12 h. The signals marked 's' are the satellite signals of the residual solvent.

Molecular models of $\mathbf{1}_2\mathbf{E}_4$[20a] and $\mathbf{1}_2\mathbf{E}^R{}_4$, calculated at the PM3 level, are shown in Figure 4b. Capsule $\mathbf{1}_2\mathbf{E}_4$, with *anti*-conformation of linker **E**, exists in $C_6D_6$ as an interconvertible mixture of (*P*)- and (*M*)-twistomers.[20b] In contrast, chiral capsule $\mathbf{1}_2\mathbf{E}^R{}_4$ tends to adopt a *bent-anti*-conformation of chiral linker $\mathbf{E}^R$, with an average $C_a$-$C_b$-$C_c$-$C_d$ torsion angle of 155° to reduce steric repulsion between the catechol and adjacent methyl groups in $\mathbf{E}^R$, and this compound was calculated to produce a (*P*)-twistomer with average dihedral angle of 65° between the resorcinol and boronic ester rings (Figure 4b and 4c). Thus, in the calculated model, the cavity size (length) of $\mathbf{1}_2\mathbf{E}^R{}_4$ is approximately 0.4 Å smaller than that of $\mathbf{1}_2\mathbf{E}_4$.

Chiral capsule $\mathbf{1}_2\mathbf{E}^R{}_4$ encapsulates guests **2** and **12** with $K_{app} = 6.93 \times 10^3\ M^{-1}$ and $\Delta\delta_G = -2.95$ ppm (AcO group) for

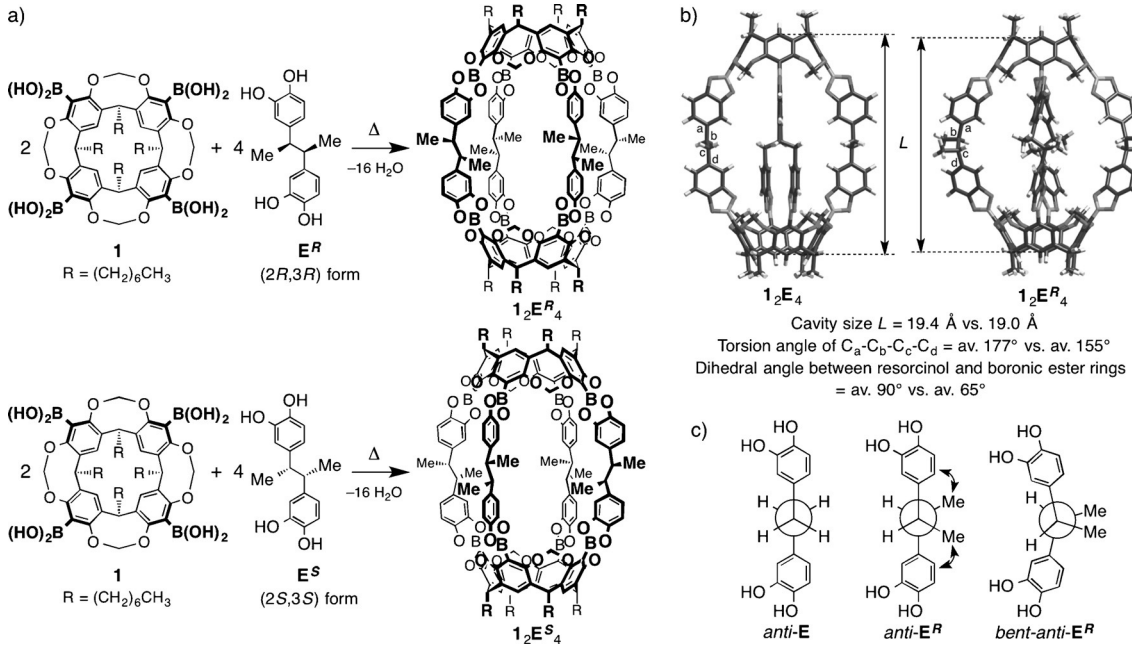


**Figure 4.** a) Formation of chiral capsules $\mathbf{1}_2\mathbf{E}^R{}_4$ and $\mathbf{1}_2\mathbf{E}^S{}_4$. b) Molecular models of $\mathbf{1}_2\mathbf{E}_4$[20a] and $\mathbf{1}_2\mathbf{E}^R{}_4$, calculated at the PM3 level. c) Schematic representation of conformations of **E** and $\mathbf{E}^R$ in capsules.

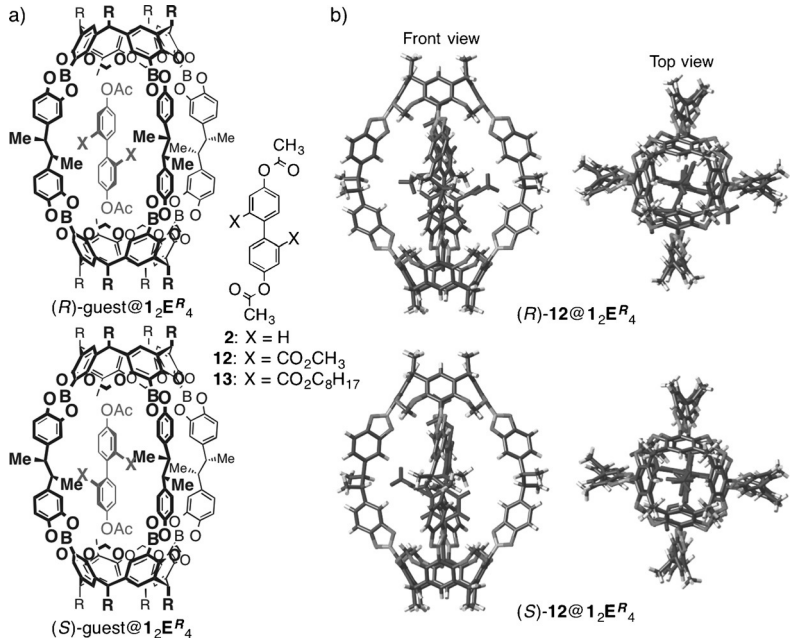


**Figure 6.** a) Schematic representation of diastereomeric encapsulation of prochiral guests **12** and **13** in $\mathbf{1}_2\mathbf{E}^R_4$. b) Molecular models of (*R*)-**12**@$\mathbf{1}_2\mathbf{E}^R_4$ and (*S*)-**12**@$\mathbf{1}_2\mathbf{E}^R_4$, calculated at the PM3 level.

ing Information), respectively. These $K_a$ values were two orders of magnitude smaller than those of **2**@$\mathbf{1}_2\mathbf{E}_4$ and **12**@$\mathbf{1}_2\mathbf{E}_4$, and these $\Delta\delta_G$ values were shifted more upfield by approximately 0.1 ppm than those of the AcO groups of **2**@$\mathbf{1}_2\mathbf{E}_4$ and **12**@$\mathbf{1}_2\mathbf{E}_4$ (Table 2, entries 2 vs. 1 and 4 vs. 3). These results also support the conclusion that the cavity size (length) of $\mathbf{1}_2\mathbf{E}^R_4$ is slightly smaller than that of $\mathbf{1}_2\mathbf{E}_4$.

In contrast to **2**@$\mathbf{1}_2\mathbf{E}^R_4$, the $^1$H NMR signal of the AcO group of **12**@$\mathbf{1}_2\mathbf{E}^R_4$ appeared as two sets of singlets (Figure 7c and 8). Furthermore, the $^1$H NMR signal of the $CO_2CH_3$ group of **12**@$\mathbf{1}_2\mathbf{E}^R_4$ also appeared as two sets of singlets at 3.40 ppm (signal-α: $\Delta\delta_G = +0.16$) and

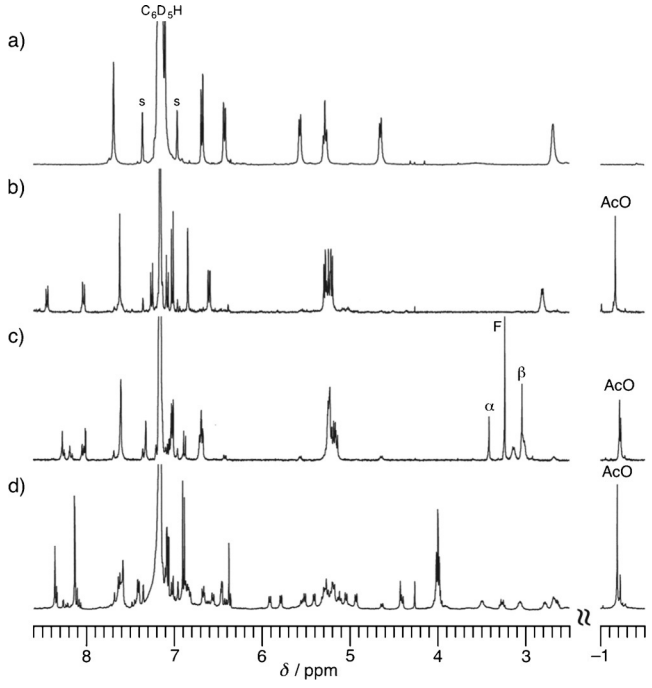


**Figure 7.** $^1$H NMR spectra (400 MHz, $C_6D_6$, 298 K) of guest@$\mathbf{1}_2\mathbf{E}^R_4$ ([$\mathbf{1}_2\mathbf{E}^R_4$] = 2.5 mM and [guest] = 3.75 mM): a) $\mathbf{1}_2\mathbf{E}^R_4$ alone; b) **2**@$\mathbf{1}_2\mathbf{E}^R_4$; c) **12**@$\mathbf{1}_2\mathbf{E}^R_4$; and d) **13**@$\mathbf{1}_2\mathbf{E}^R_4$. The signals marked 'AcO' are the acetoxy signals of the encapsulated guests. In (c), the signals marked with 'α and β' and 'F' indicate the $CO_2CH_3$ signals of the encapsulated and free **12**, respectively. The signals marked 's' are the satellite signals of the residual solvent.

**Table 2.** Comparison of $K_{app}$, $\Delta\delta_G$, and *de* values between guest@$\mathbf{1}_2\mathbf{E}_4$ and guest@$\mathbf{1}_2\mathbf{E}^R_4$ in $C_6D_6$ at 298 K.

| Entry | Capsule | Guest | $K_{app}$ [M$^{-1}$][a] | $\Delta\delta_G$ [ppm] | *de* [%][b] |
|---|---|---|---|---|---|
| 1[c] | $\mathbf{1}_2\mathbf{E}_4$ | **2** | $1.26\times10^6$ | −2.85 | |
| 2 | $\mathbf{1}_2\mathbf{E}^R_4$ | **2** | $6.93\times10^3$ | −2.95 | |
| 3[c] | $\mathbf{1}_2\mathbf{E}_4$ | **12** | $5.42\times10^5$ | −2.81 | |
| 4 | $\mathbf{1}_2\mathbf{E}^R_4$ | **12** | $4.72\times10^3$ | −2.92, −2.93 | 15 |
| 5[c] | $\mathbf{1}_2\mathbf{E}_4$ | **13** | $4.75\times10^5$ | −2.79 | |
| 6 | $\mathbf{1}_2\mathbf{E}^R_4$ | **13** | $7.31\times10^3$ | −2.90, −2.93 | 54 |

[a] Errors are within 10%. [b] *de* = diastereomeric excess for the encapsulation. [c] See Ref. [20b]. The $K_{app}$ value was measured at 313 K.

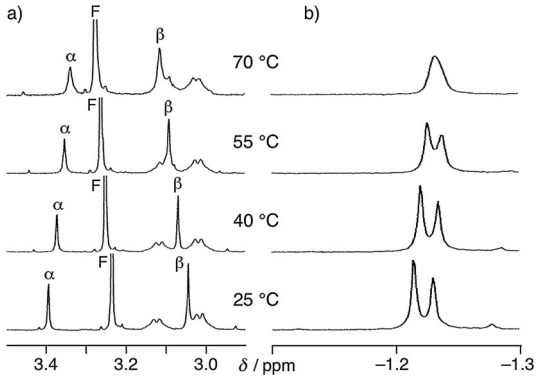


**Figure 8.** Temperature dependence of the $^1$H NMR spectra (400 MHz) of **12**@$\mathbf{1}_2\mathbf{E}^R_4$ ([$\mathbf{1}_2\mathbf{E}^R_4$] = 2.5 mM and [**12**] = 3.75 mM) in $C_6D_6$ at 25–70 °C in the region of a) the $CO_2CH_3$ groups of the encapsulated and free **12** marked with 'α and β' and 'F', respectively; and b) the AcO groups of the encapsulated **12**.

**2**@$\mathbf{1}_2\mathbf{E}^R_4$ and $K_a = 4.72\times10^3\ M^{-1}$ and $\Delta\delta_G = -2.92$ and −2.93 ppm (AcO groups) for **12**@$\mathbf{1}_2\mathbf{E}^R_4$ in $C_6D_6$ at 298 K (Figure 6). The $^1$H NMR spectra of **2**@$\mathbf{1}_2\mathbf{E}^R_4$ and **12**@$\mathbf{1}_2\mathbf{E}^R_4$ are shown in Figure 7b and 7c (Figure S23 and S24 in the Support-

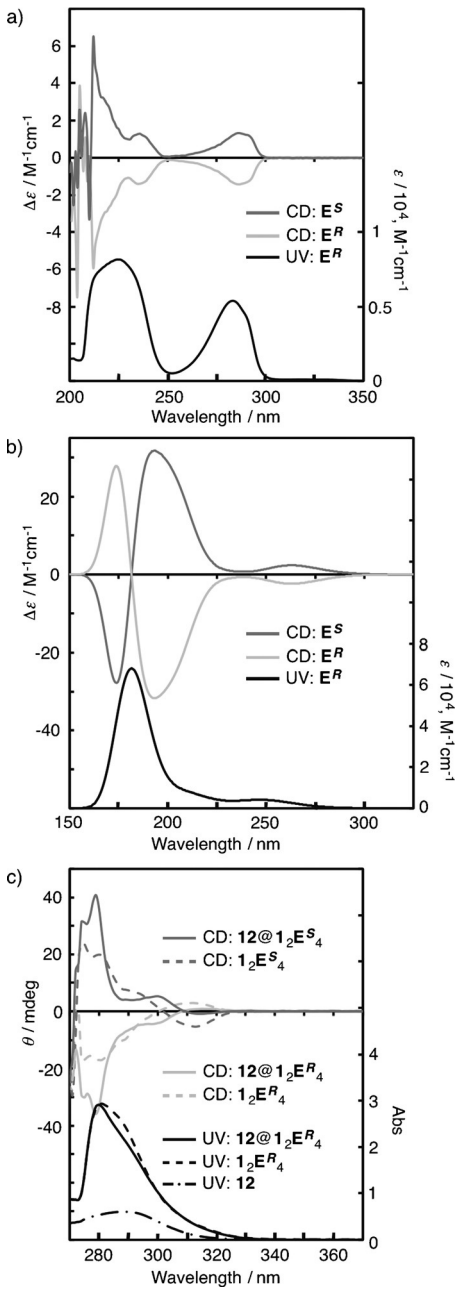


**Figure 9.** a) CD and UV/Vis spectra of $\mathbf{E}^R$ and $\mathbf{E}^S$ in THF at 25 °C (0.3 mM, $l = 0.5$ cm for CD and 1.0 cm for UV). b) Theoretical CD and UV/Vis spectra of $\mathbf{E}^R$ and $\mathbf{E}^S$, calculated with TD-DFT at the B3LYP/6-31G(d,p) level. c) CD and UV/Vis spectra of $\mathbf{1}_2\mathbf{E}^R_4$, $\mathbf{1}_2\mathbf{E}^S_4$, $\mathbf{12}@\mathbf{1}_2\mathbf{E}^R_4$, $\mathbf{12}@\mathbf{1}_2\mathbf{E}^S_4$, and **12** in $C_6H_6$ at 25 °C ($l = 0.5$ cm for CD and 1.0 cm for UV): $[\mathbf{1}_2\mathbf{E}^R_4] = [\mathbf{1}_2\mathbf{E}^S_4] = 0.05$ mM and $[\mathbf{12}] = 0.15$ mM, i.e., $[\mathbf{12}@\mathbf{1}_2\mathbf{E}^R_4] + [\mathbf{1}_2\mathbf{E}^R_4] = 0.05$ mM in total and $[\mathbf{12}@\mathbf{1}_2\mathbf{E}^S_4] + [\mathbf{1}_2\mathbf{E}^S_4] = 0.05$ mM in total.

3.04 ppm (signal-β: $\Delta\delta_G = -0.20$) relative to the signal of free **12**, which resonates at 3.24 ppm. This result indicates that chiral induction of prochiral **12** occurred upon encapsulation in the chiral nanospace of $\mathbf{1}_2\mathbf{E}^R_4$ through asymmetric suppression of rotation around the axis of the biphenyl moiety in **12**; that is, diastereomeric complexes (*R*)-$\mathbf{12}@\mathbf{1}_2\mathbf{E}^R_4$ and (*S*)-$\mathbf{12}@\mathbf{1}_2\mathbf{E}^R_4$ were produced (Figure 6). The variable-temperature $^1$H NMR spectra of $\mathbf{12}@\mathbf{1}_2\mathbf{E}^R_4$ in the region of a) the $CO_2CH_3$ groups of the encapsulated and free **12**, and b) the AcO groups of encapsulated **12** are shown in Figure 8. Although the two AcO signals of encapsulated **12** coalesced at 70 °C, the two $CO_2CH_3$ signals (α and β) of encapsulated **12** did not coalesce even at 70 °C, because the $CO_2CH_3$ groups of encapsulated **12** are placed on the chiral equatorial position of $\mathbf{1}_2\mathbf{E}^R_4$.[30] In the 2D NOESY spectra of $\mathbf{12}@\mathbf{1}_2\mathbf{E}^R_4$ (Figure S26 in the Supporting Information), exchange cross-peaks between $\mathbf{12}@\mathbf{1}_2\mathbf{E}^R_4$ and free **12** were not observed even at 70 °C, and the exchange cross-peak between the $CO_2CH_3$ signals (α and β) of $\mathbf{12}@\mathbf{1}_2\mathbf{E}^R_4$ was observed at 50 °C, but not at 25 °C. In marked contrast, rotation around the axis of **12** within $\mathbf{1}_2\mathbf{E}_4$ was fast on the NMR time-scale even at −60 °C in [$D_8$]toluene, and in the 2D NOESY spectra of $\mathbf{12}@\mathbf{1}_2\mathbf{E}_4$, exchange cross-peaks between $\mathbf{12}@\mathbf{1}_2\mathbf{E}_4$ and free **12** were observed at 50 °C, but not at 25 °C.[20b] These results clearly indicate that rotation around the axis of **12** within $\mathbf{1}_2\mathbf{E}^R_4$ as well as the exchange of **12** into and out of $\mathbf{1}_2\mathbf{E}^R_4$ are much slower than those of $\mathbf{12}@\mathbf{1}_2\mathbf{E}_4$. The diastereomeric excess (*de*) resulting from diastereomeric encapsulation selectivity of $\mathbf{12}@\mathbf{1}_2\mathbf{E}^R_4$ based on the $^1$H NMR signal integration ratios of the $CO_2CH_3$ signals (α and β) and of the two AcO signals was estimated to be 15%. Prochiral 4,4′-diacetoxy-2,2′-bis-(octoxycarbonyl)biphenyl (**13**) was also encapsulated in $\mathbf{1}_2\mathbf{E}^R_4$ with $K_{app} = 7.31 \times 10^3\ M^{-1}$ and $\Delta\delta_G = -2.90$ and $-2.93$ ppm (AcO group) (Figure 7d and Table 2, entry 6). It is known that, in contrast to $\mathbf{12}@\mathbf{1}_2\mathbf{E}_4$, rotation around the axis of **13** within $\mathbf{1}_2\mathbf{E}_4$ is inhibited at 25 °C in $C_6D_6$[20b] because the $CO_2C_8H_{17}$ groups of encapsulated **13** protrude from the equatorial windows of $\mathbf{1}_2\mathbf{E}_4$. This is also the case for $\mathbf{13}@\mathbf{1}_2\mathbf{E}^R_4$. Therefore, the diastereomeric encapsulation selectivity of $\mathbf{13}@\mathbf{1}_2\mathbf{E}^R_4$ (*de* = 54%) was greater than that of $\mathbf{12}@\mathbf{1}_2\mathbf{E}^R_4$. At this stage, it is not easy to establish which enantiomer of (*R*)- or (*S*)-guest is more favorably encapsulated in $\mathbf{1}_2\mathbf{E}^R_4$, and further studies are required in this regard.

### Chiral induction of prochiral biphenyl guest: a CD study

Circular dichroism (CD) spectroscopy was used to examine further the chiral induction of prochiral biphenyl guest upon encapsulation in chiral capsules $\mathbf{1}_2\mathbf{E}^R_4$ and $\mathbf{1}_2\mathbf{E}^S_4$ (Figure 9). The chiral linkers $\mathbf{E}^R$ and $\mathbf{E}^S$ in THF showed CD spectra that were reciprocal, and the UV/Vis absorption maxima of $\mathbf{E}^R$ were observed at 212–225 and 284 nm (Figure 9a). The CD signals corresponding to absorption at 212–225 nm were not definitive because the shorter wavelength region below 220 nm overlapped with absorption by THF. Nevertheless, the split CD signals in the region were deduced from the theoretical CD calculated with TD-DFT at the B3LYP/6-31G(d,p) level (Figure 9a vs. 9b). The CD spectra of $\mathbf{E}^R$ and $\mathbf{E}^S$ also showed mirror image signals at 283 nm in addition to the split CD signals described above. The CD signal at approximately 280 nm constitutes a valuable CD probe that can be used to determine chiral induction of the prochiral biphenyl guest (see below).

The CD study of $\mathbf{1}_2\mathbf{E}^R_4$ and $\mathbf{12}@\mathbf{1}_2\mathbf{E}^R_4$ was carried out in benzene to maintain guest encapsulation; therefore, it was not possible to study the shorter wavelength region below 270 nm, which overlaps with the absorption of the solvent.

The CD spectra of $\mathbf{1}_2\mathbf{E}^R_4$ and $\mathbf{1}_2\mathbf{E}^S_4$ in benzene (0.05 mM) showed mirror image signals with CD maxima at 273 and 283 nm, and exhibited the same CD signs relative to those of $\mathbf{E}^R$ and $\mathbf{E}^S$, respectively (Figure 9c). The solution of $\mathbf{12}@\mathbf{1}_2\mathbf{E}^R_4$ for the CD and UV/Vis measurements ($[\mathbf{1}_2\mathbf{E}^R_4]=0.05$ mM and $[\mathbf{12}]=0.15$ mM in $C_6H_6$, i.e., $[\mathbf{12}@\mathbf{1}_2\mathbf{E}^R_4]+[\mathbf{1}_2\mathbf{E}^R_4]=0.05$ mM in total) contains $\mathbf{12}@\mathbf{1}_2\mathbf{E}^R_4$ (38%), free $\mathbf{1}_2\mathbf{E}^R_4$ (62%), and excess free **12**, calculated based on the $K_{app}$ value. At wavelengths longer than 270 nm, the UV/Vis absorption maxima of $\mathbf{E}^R$ (284 nm) in THF, and $\mathbf{1}_2\mathbf{E}^R_4$ (281 nm), the solution containing $\mathbf{12}@\mathbf{1}_2\mathbf{E}^R_4$ (280 nm), and free **12** (289 nm) in benzene appeared in a similar wavelength region (Figure 9c). Therefore, the origin of the CD signals of $\mathbf{12}@\mathbf{1}_2\mathbf{E}^R_4$ is complex. The CD spectra of a solution containing $\mathbf{12}@\mathbf{1}_2\mathbf{E}^R_4$ and $\mathbf{12}@\mathbf{1}_2\mathbf{E}^S_4$ showed mirror image signals and exhibited the same CD signs relative to those of $\mathbf{1}_2\mathbf{E}^R_4$ and $\mathbf{1}_2\mathbf{E}^S_4$, respectively. Notably, $\mathbf{12}@\mathbf{1}_2\mathbf{E}^R_4$ and $\mathbf{12}@\mathbf{1}_2\mathbf{E}^S_4$ showed an approximate twofold increase in the CD signal intensity at around 280 nm, compared with $\mathbf{1}_2\mathbf{E}^R_4$ and $\mathbf{1}_2\mathbf{E}^S_4$, respectively (Figure 9c). In contrast, there was almost no increase in the CD signal intensity of achiral-$\mathbf{2}@\mathbf{1}_2\mathbf{E}^S_4$ relative to that of $\mathbf{1}_2\mathbf{E}^S_4$ (Figure 10a). These results strongly support the

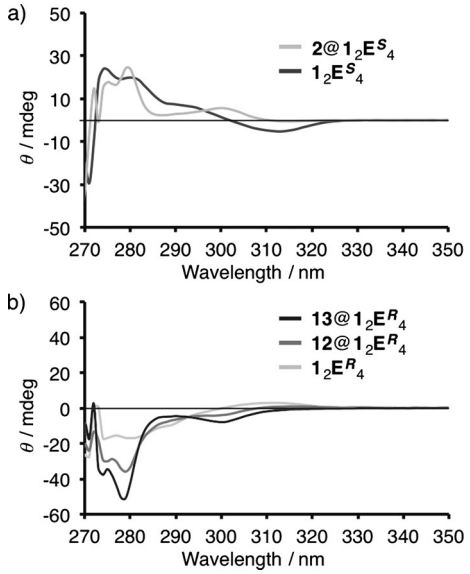


**Figure 10.** CD spectra of a) $\mathbf{1}_2\mathbf{E}^S_4$ and $\mathbf{2}@\mathbf{1}_2\mathbf{E}^S_4$; and b) $\mathbf{1}_2\mathbf{E}^R_4$, $\mathbf{12}@\mathbf{1}_2\mathbf{E}^R_4$, and $\mathbf{13}@\mathbf{1}_2\mathbf{E}^R_4$ in $C_6H_6$ at 25 °C ($l=0.5$ cm and [guest@chiral-capsule] + [chiral-capsule] = 0.05 mM in total and [guest] = 0.15 mM).

idea of chiral induction of prochiral **12** upon encapsulation in $\mathbf{1}_2\mathbf{E}^R_4$ and $\mathbf{1}_2\mathbf{E}^S_4$. The increase of the CD signal intensity of $\mathbf{12}@\mathbf{1}_2\mathbf{E}^R_4$ would arise from an exciton coupling between chiral **12** and $\mathbf{1}_2\mathbf{E}^R_4$, but not from a CD signal of chiral **12** alone, because the absorbance of **12** is much smaller than that of $\mathbf{1}_2\mathbf{E}^R_4$ (Figure 9c). Furthermore, $\mathbf{13}@\mathbf{1}_2\mathbf{E}^R_4$ showed an approximate threefold increase in the CD signal intensity at around 280 nm, compared with that of $\mathbf{1}_2\mathbf{E}^R_4$ (Figure 10b). This dramatic increase in the CD signal intensity of $\mathbf{13}@\mathbf{1}_2\mathbf{E}^R_4$ compared with those of $\mathbf{12}@\mathbf{1}_2\mathbf{E}^R_4$ and $\mathbf{1}_2\mathbf{E}^R_4$ arises from larger diastereomeric encapsulation selectivity for $\mathbf{13}@\mathbf{1}_2\mathbf{E}^R_4$ ($de=54$%) than that for $\mathbf{12}@\mathbf{1}_2\mathbf{E}^R_4$ ($de=15$%), as mentioned in the $^1$H NMR study.

## Conclusion

We have demonstrated the self-assembly of two molecules of cavitand tetraboronic acid **1** and four molecules of various bis(catechol) linkers **P**, **B**, **L**, $\mathbf{E}^R$, and $\mathbf{E}^S$ into capsules $\mathbf{1}_2\mathbf{P}_4$, $\mathbf{1}_2\mathbf{B}_4$, $\mathbf{1}_2\mathbf{L}_4$, $\mathbf{1}_2\mathbf{E}^R_4$, and $\mathbf{1}_2\mathbf{E}^S_4$, respectively, through the formation of eight dynamic boronic ester bonds. The following two features are particularly noteworthy in this study. 1) Each capsule has a different cavity size that depends on the linkers, and shows particular guest encapsulation selectivity. Capsules $\mathbf{1}_2\mathbf{B}_4$ and $\mathbf{1}_2\mathbf{L}_4$, with more expanded cavity than previously reported $\mathbf{1}_2\mathbf{E}_4$, were able to encapsulate larger guests such as **3** and **9**, respectively, which are inaccessible for $\mathbf{1}_2\mathbf{E}_4$. The capsules can also clearly discriminate between functional groups of a guest. 2) Chiral capsules $\mathbf{1}_2\mathbf{E}^R_4$ and $\mathbf{1}_2\mathbf{E}^S_4$ induced supramolecular chirality with respect to prochiral biphenyl guests **12** and **13** by diastereomeric encapsulation through asymmetric suppression or inhibition of rotation around the axis of the biphenyl moiety of the guests upon encapsulation in the chiral nanospace. Thus, the self-assembled boronic ester cavitand capsules show unique properties that depend on the characteristics of the bis(catechol) linkers. Further modifications of the bis(catechol) linker and cavitand tetraboronic acid are expected to endow this type of capsule with characteristics that should help in the development of functional materials, which would constitute an important advance in supramolecular nanospace chemistry.

## Experimental Section

### Typical procedure for capsule formation: capsule $\mathbf{1}_2\mathbf{E}^R_4$

A suspension of $\mathbf{1}\cdot OEt_2$ (50.0 mg, 42.4 μmol) and $\mathbf{E}^R$ (23.3 mg, 84.9 μmol, 2 equiv) in $CDCl_3$ (8.5 mL) was stirred at 50 °C for 12 h under Ar. The $^1$H NMR spectrum of the resulting homogeneous solution showed the quantitative formation of $\mathbf{1}_2\mathbf{E}^R_4$. After evaporation of solvent, the residue was dried in vacuo at RT for 5 h. The resulting solid was precipitated from benzene–hexane to give $\mathbf{1}_2\mathbf{E}^R_4$ (62.1 mg, 97% yield) as a white solid. $^1$H NMR (400 MHz, $CDCl_3$, 298 K): $\delta=7.37$ (s, 8H; $H_D$), 7.25 (s, 8H; $H_c$), 7.06 (d, $J=7.8$ Hz, 8H; $H_a$), 6.70 (d, $J=7.8$ Hz, 8H; $H_b$), 5.72 (d, $J=7.3$ Hz, 8H; $H_B$), 4.89 (t, $J=7.8$ Hz, 8H; $H_C$), 4.67 (d, $J=7.3$ Hz, 8H; $H_A$), 3.04 (m, 8H; $H_d$), 2.30 (m, 16H), 1.25–1.55 (m, 80H), 1.21 (d, $J=5.9$ Hz, 24H; $H_e$), 0.92 ppm (t, $J=6.8$ Hz, 24H); $^1$H NMR (400 MHz, $C_6D_6$, 298 K): $\delta=7.69$ (s, 8H; $H_D$), 7.10 (s, 8H; $H_c$), 6.68 (d, $J=7.8$ Hz, 8H; $H_a$), 6.42 (d, $J=7.8$ Hz, 8H; $H_b$), 5.55 (d, $J=7.3$ Hz, 8H; $H_B$), 5.27 (t, $J=7.8$ Hz, 8H; $H_C$), 4.64 (d, $J=7.3$ Hz, 8H; $H_A$), 2.67 (m, 8H; $H_d$), 2.30 (m, 16H), 1.20–1.40 (m, 80H), 1.13 (d, $J=4.4$ Hz, 24H; $H_e$), 0.93 ppm (t, $J=6.8$ Hz, 24H). The signal assignments are shown in Figure S22 in the Supporting Information.

## *Acknowledgements*

We thank Daicel Corporation CPI Company for the chiral AY-H column, Professor Toshiyuki Kan and Dr. Tomohiro Asakawa (University of Shizuoka) for optical rotation measurements, and Ayumi Oishi for experimental assistance. This work was supported in part by a Grant-in-Aid from JSPS (no. 25288034).

**Keywords:** cavitands · drug delivery · host–guest systems · self-assembly · supramolecular chemistry

[1] a) D. J. Cram, J. M. Cram, *Container Molecules and Their Guests*, Royal Society of Chemistry, Cambridge, **1994**; b) A. Jasat, J. C. Sherman, *Chem. Rev.* **1999**, *99*, 931 – 967; c) R. Warmuth, J. Yoon, *Acc. Chem. Res.* **2001**, *34*, 95 – 105; d) J. C. Sherman, *Chem. Commun.* **2003**, 1617 – 1623.

[2] a) J. Rebek, Jr., *Acc. Chem. Res.* **2009**, *42*, 1660 – 1668; b) K. Kobayashi, M. Yamanaka, *Chem. Soc. Rev.* **2015**, *44*, 449 – 466, and references therein.

[3] a) P. Jacopozzi, E. Dalcanale, *Angew. Chem. Int. Ed. Engl.* **1997**, *36*, 613 – 615; *Angew. Chem.* **1997**, *109*, 665 – 667; b) O. D. Fox, N. K. Dalley, R. G. Harrison, *J. Am. Chem. Soc.* **1998**, *120*, 7111 – 7112; c) O. D. Fox, M. G. B. Drew, P. D. Beer, *Angew. Chem. Int. Ed.* **2000**, *39*, 135 – 140; *Angew. Chem.* **2000**, *112*, 139 – 144; d) R. Pinalli, V. Cristini, V. Sottili, S. Geremia, M. Campagnolo, A. Caneschi, E. Dalcanale, *J. Am. Chem. Soc.* **2004**, *126*, 6516 – 6517; e) K. Kobayashi, Y. Yamada, M. Yamanaka, Y. Sei, K. Yamaguchi, *J. Am. Chem. Soc.* **2004**, *126*, 13896 – 13897; f) T. Haino, M. Kobayashi, M. Chikaraishi, Y. Fukazawa, *Chem. Commun.* **2005**, 2321 – 2323; g) S. J. Park, D. M. Shin, S. Sakamoto, K. Yamaguchi, Y. K. Chung, M. S. Lah, J.-I. Hong, *Chem. Eur. J.* **2005**, *11*, 235 – 241.

[4] G. V. Oshovsky, D. N. Reinhoudt, W. Verboom, *J. Am. Chem. Soc.* **2006**, *128*, 5270 – 5278.

[5] C. L. Gibb, B. C. Gibb, *J. Am. Chem. Soc.* **2004**, *126*, 11408 – 11409.

[6] For reviews of dynamic covalent chemistry, see: a) S. J. Rowan, S. J. Cantrill, G. R. L. Cousins, J. K. M. Sanders, J. F. Stoddart, *Angew. Chem. Int. Ed.* **2002**, *41*, 898 – 952; *Angew. Chem.* **2002**, *114*, 938 – 993; b) P. T. Corbett, J. Leclaire, L. Vial, K. R. West, J.-L. Wietor, J. K. M. Sanders, S. Otto, *Chem. Rev.* **2006**, *106*, 3652 – 3711; c) F. B. L. Cougnon, J. K. M. Sanders, *Acc. Chem. Res.* **2012**, *45*, 2211 – 2221; d) J. Li, P. Nowak, S. Otto, *J. Am. Chem. Soc.* **2013**, *135*, 9222 – 9239.

[7] For reviews of self-assembled capsules based on dynamic covalent chemistry, see: a) M. Mastalerz, *Angew. Chem. Int. Ed.* **2010**, *49*, 5042 – 5053; *Angew. Chem.* **2010**, *122*, 5164 – 5175; b) N. M. Rue, J. Sun, R. Warmuth, *Isr. J. Chem.* **2011**, *51*, 743 – 768; c) G. Zhang, M. Mastalerz, *Chem. Soc. Rev.* **2014**, *43*, 1934 – 1947.

[8] a) S. Ro, S. J. Rowan, A. R. Pease, D. J. Cram, J. F. Stoddart, *Org. Lett.* **2000**, *2*, 2411 – 2414; b) X. Liu, Y. Liu, G. Li, R. Warmuth, *Angew. Chem. Int. Ed.* **2006**, *45*, 901 – 904; *Angew. Chem.* **2006**, *118*, 915 – 918; c) X. Liu, R. Warmuth, *J. Am. Chem. Soc.* **2006**, *128*, 14120 – 14127.

[9] J. Sun, B. O. Patrick, J. C. Sherman, *Tetrahedron* **2009**, *65*, 7296 – 7302.

[10] For reviews of supramolecular architectures based on dynamic boronic ester bonds, see: a) N. Fujita, S. Shinkai, T. D. James, *Chem. Asian J.* **2008**, *3*, 1076 – 1091; b) R. Nishiyabu, Y. Kubo, T. D. James, J. S. Fossey, *Chem. Commun.* **2011**, *47*, 1124 – 1150; c) Y. Kubo, R. Nishiyabu, T. D. James, *Chem. Commun.* **2015**, *51*, 2005 – 2020.

[11] For self-assembled capsules based on dynamic boronic ester bonds, see: a) N. Iwasawa, H. Takahagi, *J. Am. Chem. Soc.* **2007**, *129*, 7754 – 7755; b) K. Kataoka, T. D. James, Y. Kubo, *J. Am. Chem. Soc.* **2007**, *129*, 15126 – 15127; c) B. Içli, N. Christinat, J. Tönnemann, C. Schüttler, R. Scopelliti, K. Severin, *J. Am. Chem. Soc.* **2009**, *131*, 3154 – 3155; d) G. Zhang, O. Presly, F. White, I. M. Oppel, M. Mastalerz, *Angew. Chem. Int. Ed.* **2014**, *53*, 1516 – 1520; *Angew. Chem.* **2014**, *126*, 1542 – 1546; e) G. Zhang, O. Presly, F. White, I. M. Oppel, M. Mastalerz, *Angew. Chem. Int. Ed.* **2014**, *53*, 5126 – 5130; *Angew. Chem.* **2014**, *126*, 5226 – 5230; f) S. Klotzbach, T. Scherpf, F. Beuerle, *Chem. Commun.* **2014**, *50*, 12454 – 12457; g) K. Ono, K. Johmoto, N. Yasuda, H. Uekusa, S. Fujii, M. Kiguchi, N. Iwasawa, *J. Am. Chem. Soc.* **2015**, *137*, 7015 – 7018.

[12] For chiral molecular recognition of racemic guests by using covalently bound chiral capsules (hemicarcerands), see: a) J. Canceill, L. Lacombe, A. Collet, *J. Am. Chem. Soc.* **1985**, *107*, 6993 – 6996; b) J. K. Judice, D. J. Cram, *J. Am. Chem. Soc.* **1991**, *113*, 2790 – 2791; c) J. Costante-Crassous, T. J. Marrone, J. M. Briggs, J. A. McCammon, A. Collet, *J. Am. Chem. Soc.* **1997**, *119*, 3818 – 3823; d) J. Yoon, D. J. Cram, *J. Am. Chem. Soc.* **1997**, *119*, 11796 – 11806; e) B. S. Park, C. B. Knobler, C. N. Eid, Jr., R. Warmuth, D. J. Cram, *Chem. Commun.* **1998**, 55 – 56; f) A. Bouchet, T. Brotin, M. Linares, H. Ågren, D. Cavagnat, T. Buffeteau, *J. Org. Chem.* **2011**, *76*, 4178 – 4181.

[13] For reviews of self-assembled chiral capsules, see: a) M. A. Mateos-Timoneda, M. Crego-Calama, D. N. Reinhoudt, *Chem. Soc. Rev.* **2004**, *33*, 363 – 372; b) A. Scarso, J. Rebek, Jr., *Top. Curr. Chem.* **2006**, *265*, 1 – 46; c) G. Seeber, B. E. F. Tiedemann, K. N. Raymond, *Top. Curr. Chem.* **2006**, *265*, 147 – 183.

[14] For chiral molecular recognition of racemic guests by using self-assembled chiral capsules, see: a) R. K. Castellano, B. H. Kim, J. Rebek, Jr., *J. Am. Chem. Soc.* **1997**, *119*, 12671 – 12672; b) R. K. Castellano, C. Nuckolls, J. Rebek, Jr., *J. Am. Chem. Soc.* **1999**, *121*, 11156 – 11163; c) J. M. Rivera, T. Martin, J. Rebek, Jr., *J. Am. Chem. Soc.* **2001**, *123*, 5213 – 5220; d) D. Fiedler, D. H. Leung, R. G. Bergman, K. N. Raymond, *J. Am. Chem. Soc.* **2004**, *126*, 3674 – 3675; e) T. Haino, M. Kobayashi, Y. Fukazawa, *Chem. Eur. J.* **2006**, *12*, 3310 – 3319; f) C. J. Hastings, M. D. Pluth, S. M. Biros, R. G. Bergman, K. N. Raymond, *Tetrahedron* **2008**, *64*, 8362 – 8367; g) A. Szumna, *Chem. Eur. J.* **2009**, *15*, 12381 – 12388.

[15] a) D. J. Cram, M. T. Blanda, K. Paek, C. B. Knobler, *J. Am. Chem. Soc.* **1992**, *114*, 7765 – 7773; b) T. A. Robbins, C. B. Knobler, D. R. Bellew, D. J. Cram, *J. Am. Chem. Soc.* **1994**, *116*, 111 – 122; c) R. G. Chapman, J. C. Sherman, *J. Am. Chem. Soc.* **1999**, *121*, 1962 – 1963; d) K. Paek, H. Ihm, S. Yun, H. C. Lee, *Tetrahedron Lett.* **1999**, *40*, 8905 – 8909; e) R. G. Chapman, J. C. Sherman, *J. Org. Chem.* **2000**, *65*, 513 – 516.

[16] a) A. Ikeda, H. Udzu, Z. Zhong, S. Shinkai, S. Sakamoto, K. Yamaguchi, *J. Am. Chem. Soc.* **2001**, *123*, 3872 – 3877; b) Y. Tsunoda, K. Fukuta, T. Imamura, R. Sekiya, T. Furuyama, N. Kobayashi, T. Haino, *Angew. Chem. Int. Ed.* **2014**, *53*, 7243 – 7247; *Angew. Chem.* **2014**, *126*, 7371 – 7375.

[17] a) Y. Nishioka, T. Yamaguchi, M. Kawano, M. Fujita, *J. Am. Chem. Soc.* **2008**, *130*, 8160 – 8161; b) C. J. Brown, R. G. Bergman, K. N. Raymond, *J. Am. Chem. Soc.* **2009**, *131*, 17530 – 17531.

[18] a) T. Amaya, J. Rebek, Jr., *J. Am. Chem. Soc.* **2004**, *126*, 6216 – 6217; b) M. P. Schramm, J. Rebek, Jr., *New J. Chem.* **2008**, *32*, 794 – 796.

[19] a) P. Skowronek, J. Gawronski, *Org. Lett.* **2008**, *10*, 4755 – 4758; b) D. Xu, R. Warmuth, *J. Am. Chem. Soc.* **2008**, *130*, 7520 – 7521; c) T. Mitra, K. E. Jelfs, M. Schmidtmann, A. Ahmed, S. Y. Chong, D. J. Adams, A. I. Cooper, *Nat. Chem.* **2013**, *5*, 276 – 281.

[20] a) N. Nishimura, K. Kobayashi, *Angew. Chem. Int. Ed.* **2008**, *47*, 6255 – 6258; *Angew. Chem.* **2008**, *120*, 6351 – 6354; b) N. Nishimura, K. Yoza, K. Kobayashi, *J. Am. Chem. Soc.* **2010**, *132*, 777 – 790; c) N. Nishimura, K. Kobayashi, *J. Org. Chem.* **2010**, *75*, 6079 – 6085; d) Y. Hirumi, K. Tamaki, T. Namikawa, K. Kamada, M. Mitsui, K. Suzuki, K. Kobayashi, *Chem. Asian J.* **2014**, *9*, 1282 – 1290; e) M. Mitsui, K. Higashi, R. Takahashi, Y. Hirumi, K. Kobayashi, *Photochem. Photobiol. Sci.* **2014**, *13*, 1130 – 1136.

[21] For cavity-expanded self-assembled capsules based on hydrogen bonds or metal-coordination bonds, see: a) Y. L. Cho, D. M. Rudkevich, J. Rebek, Jr., *J. Am. Chem. Soc.* **2000**, *122*, 9868 – 9869; b) M. Yamanaka, Y. Yamada, Y. Sei, K. Yamaguchi, K. Kobayashi, *J. Am. Chem. Soc.* **2006**, *128*, 1531 – 1539; c) D. Ajami, J. Rebek, Jr., *J. Am. Chem. Soc.* **2006**, *128*, 5314 – 5315; d) M. Yamanaka, K. Ishii, Y. Yamada, K. Kobayashi, *J. Org. Chem.* **2006**, *71*, 8800 – 8806; e) K. Ono, M. Yoshizawa, T. Kato, K. Watanabe, M. Fujita, *Angew. Chem. Int. Ed.* **2007**, *46*, 1803 – 1806; *Angew. Chem.* **2007**, *119*, 1835 – 1838; f) C. B. Aakeröy, A. Rajbanshi, J. Desper, *Chem. Commun.* **2011**, *47*, 11411 – 11413; g) D. Samanta, P. S. Mukherjee, *Chem. Eur. J.* **2014**, *20*, 12483 – 12492.

[22] For cavity-expanded self-assembled capsules based on dynamic covalent bonds, see: a) J. Sun, R. Warmuth, *Chem. Commun.* **2011**, *47*, 9351 – 9353; b) A. Granzhan, C. Schouwey, T. Riis-Johannessen, R. Scopelliti, K. Severin, *J. Am. Chem. Soc.* **2011**, *133*, 7106 – 7115; c) M. W. Schneider, I. M. Oppel, M. Mastalerz, *Chem. Eur. J.* **2012**, *18*, 4156 – 4160; d) M. Brutschy, M. W. Schneider, M. Mastalerz, S. R. Waldvogel, *Adv. Mater.* **2012**, *24*, 6049 – 6052; e) K. Acharyya, S. Mukherjee, P. S. Mukherjee, *J. Am. Chem. Soc.* **2013**, *135*, 554 – 557; f) K. E. Jelfs, E. G. B. Eden, J. L. Culshaw, S. Shakespeare, E. O. Pyzer-Knapp, H. P. G. Thompson, J. Bacsa, G. M. Day, D. J. Adams, A. I. Cooper, *J. Am. Chem. Soc.* **2013**, *135*, 9307 – 9310; g) A. Asadi, D. Ajami, J. Rebek, Jr., *Chem. Commun.* **2014**, *50*, 533 – 535.

[23] R. W. McDonald, W. Bunjobpon, T. Liu, S. Fessler, O. E. Pardo, I. K. A. Freer, M. Glaser, M. J. Seckl, D. J. Robins, *Anti-Cancer Drug Des.* **2001**, *16*, 261 – 270.

[24] The reaction of a 2:4 mixture of **1** with 2,3,6,7-tetrahydroxyphenanthrene, 3,3′,4,4′-tetrahydroxybiphenyl, or bis(3,4-dihydroxyphenyl)acetylene as a rigid bis(catechol) linker in $CDCl_3$ at 50 °C did not give a single species of the corresponding capsule, wherein a mixture of less soluble unidentified oligomers was mainly formed.

[25] Large $K_{app}$ values of capsules with guests were estimated by competitive encapsulation experiments with a standard guest. Details are given in the Supporting Information.

[26] The guest length of 4,4′-bis(1-propynyl)biphenyl (**14**) ($l = 15.16$ Å) is longer than **2** ($l = 14.35$ Å), where $l = C\cdots C$ atomic distance between the terminal $CH_3$ groups, calculated at the B3LYP/6-31G(d) level. It is known that the 1-propynyl group as well as the acetoxy group is a good functional group for guest encapsulation in a cavitand-based capsule.[27] For guest@$\mathbf{1}_2\mathbf{E}_4$, the $K_{app}$ of **14**@$\mathbf{1}_2\mathbf{E}_4$ ($K_{app} = 507\ M^{-1}$) was much smaller than **2**@$\mathbf{1}_2\mathbf{E}_4$ ($K_{app} = 1.26\times10^6\ M^{-1}$), whereas the negative $\Delta\delta_G$ value (upfield shift value) of **14**@$\mathbf{1}_2\mathbf{E}_4$ ($\Delta\delta_G = -3.18$ ppm) was greater than **2**@$\mathbf{1}_2\mathbf{E}_4$ ($\Delta\delta_G = -2.85$ ppm).[20b] This result clearly indicates that the size of **14** is closer to the cavity size of $\mathbf{1}_2\mathbf{E}_4$ than **2**. In the present work, **14** was not encapsulated in $\mathbf{1}_2\mathbf{P}_4$, because the size of **14** is too large for the cavity size of $\mathbf{1}_2\mathbf{P}_4$. These results also support the conclusion that the cavity size (length) of $\mathbf{1}_2\mathbf{P}_4$ is somewhat smaller than that of $\mathbf{1}_2\mathbf{E}_4$.

[27] K. Ichihara, H. Kawai, Y. Togari, E. Kikuta, H. Kitagawa, S. Tsuzuki, K. Yoza, M. Yamanaka, K. Kobayashi, *Chem. Eur. J.* **2013**, *19*, 3685 – 3692.

[28] R. Holzwarth, R. Bartsch, Z. Cherkaoui, G. Solladié, *Chem. Eur. J.* **2004**, *10*, 3931 – 3935.

[29] S. Ito, K. Ono, N. Iwasawa, *J. Am. Chem. Soc.* **2012**, *134*, 13962 – 13965.

[30] This different behavior, namely, the coalescence of only the two AcO signals, would contain the rotation of the AcO group on the AcO–biphenyl bond at higher temperature, which is different from the chirality inversion.

Received: May 2, 2015
Published online on August 3, 2015

 